Comparisons between trumpet models using numerical continuation methods

Margaret Hopkins

Music Technology Area, Department of Music Research
Schulich School of Music
McGill University
Montréal, Québec, Canada

August 15, 2023

A thesis presented for the degree of Masters of Arts in Music Technology

Abstract

This thesis describes the use of numerical continuation methods to analyze the behavior of a modeled trumpet-player system, and to make comparisons between the instruments based on parameters that are relevant to players. The acoustic impedances of four B$^\flat$ trumpets were measured, and modal parameters were derived to describe each measured impedance. The modal impedance parameters were then incorporated into a physical model representing the player-trumpet system. Linear stability analysis (LSA) was used to refine the lip frequency parameter used, and then the system was studied using numerical continuation methods to determine how the mouthpiece pressure varies with the blowing pressure. Bifurcation diagrams of downstream mouthpiece pressure versus upstream blowing pressure were generated using the numerical continuation software Manlab, and it was found that all four trumpets displayed subcritical, or inverse, Hopf bifurcations at the note onset. This means that each instrument displayed hysteresis behavior, so that the minimum onset blowing pressure and dynamic were higher than the extinction blowing pressure and dynamic. The location of the Hopf bifurcation point, the mouthpiece pressure at an estimate of the players' maximum blowing pressure, and location of the fold, where the oscillating solution becomes extinct as the blowing pressure is reduced, were determined for each instrument. The locations of these landmarks were used to make

conjectures about the amount of blowing pressure needed to begin a note, the maximum and minimum dynamics of the instrument, the dynamic range, and the amplitude of the hysteresis for each instrument. A small-scale perceptual trial was conducted to determine whether players could perceive these differences, and whether their observations agreed with the conjectures made based on the results from numerical continuation.

Abrégé

Cette thèse présente l'utilisation des méthodes de continuation numérique pour analyser le comportement d'un modèle d'un système trompette-joueur et pour comparer les instruments par des paramètres pertinents aux joueurs. Les impédances acoustiques de quatre trompettes en si bémol étaient mesurées, et les paramètres modales étaient calculés pour décrire chaque impédance mesuré. À la suite, les paramètres modales d'impédance étaient incorporés dans un modèle physique qui représentait le système trompette-joueur. L'analyse de stabilité linéaire (ASL) était utilisée pour ajuster les paramètres de la fréquence des lèvres, ensuite le système était examiné avec les méthodes de continuation numérique pour déterminer comment la pression de l'embouchure variait avec la pression du souffle. Des diagrammes de bifurcation de la pression de l'embouchure versus la pression du souffle étaient créés avec le logiciel Manlab, et on découvre que les quatre trompettes avaient des bifurcation de Hopf subcritique, ou inverse, à l'attaque. Cela signifie que chaque instrument avait le comportement d' hystérésis, donc la pression du souffle et le volume minimum pour l'attaque étaient plus hauts que la pression du souffle et le volume de l'extinction. L'emplacement de la bifurcation de Hopf, la valeur de la pression de l'embouchure à la pression maximale du souffle, et la location du pli où la solution oscillant disparaît à la réduction de la pression du souffle ont été calculés pour chaque instrument. L'emplacement des ces repères étaient

utilisés pour formuler des conjectures à propos de la valeur de la pression du souffle requise pour commencer une note, les sons minimales et maximales, la gamme des nuances, et l'ampleur de l'hystérésis pour chaque instrument. Un essai perceptif à petite échelle était mené pour évaluer si des joueurs pouvaient distinguer ces différences et si leurs observations correspondaient avec les conjectures fondées sur les résultats de la continuation numérique.

Acknowledgements

I would like to extend a warm thank you to Dr. Gary Scavone for supervising me and guiding me throughout my degree and through the completion of this thesis, to Dr. Vincent Fréour for assisting me with the use of the software Manlab and helping with clarification and interpretation of results, and to the participants of my perceptual trial for contributing their time and expertise. Thank you as well to my colleagues in CAML, including the individuals who allowed me to use their instruments both for impedance measurements and in my perceptual trial, to all the professors of the McGill Music Technology Department for teaching me the skills necessary to complete this degree, and to the Centre for Interdisciplinary Research in Music Media and Technology (CIRMMT) for the use of laboratory spaces and equipment. Finally, thank you to my family and friends, and to the eZone for supporting me throughout this degree.

Contents

List of Figures

List of Tables

Chapter 1

Introduction

1.1 Motivation

The design of trumpets, like other brass instruments, has traditionally relied on work by artisans and manufacturers without a basis in acoustical science. Though results and techniques from acoustical science may help to make instrument design more efficient and affordable, these resources have not often been implemented by manufacturers.

Various prior research has been conducted to classify acoustical parameters according to their influence on a performer's experience of playing an instrument. These parameters are then used to make comparisons between measured representations of different instruments and to make conjectures based on these comparisons about the instruments' playing characteristics. For example, Elie et al. [2012] use acoustical parameters to classify classical guitars according to parameters that can be influenced by the manufacturer, Mansour et al. [2015] use bridge admittances to classify models of guitars and compare their results with descriptions from the manufacturer, and Woodhouse [1993] classifies

violins by parameters related to "playability," including a parameter for the minimum bow force required to begin a note.

One assessment criterion for wind instruments that is both relevant to players and can be investigated through numerical methods is how the amplitude of oscillation varies with blowing pressure, often referred to by players as the "response" of the instrument. This encompasses threshold factors such as minimum onset pressure and extinction pressure, as well as how the mouthpiece pressure, related to the perceived loudness of the instrument, varies as the player increases and decreases their blowing pressure. The response to varying levels of blowing pressure has been investigated for woodwind instruments in [Dalmont et al., 2005] and [Colinot et al., 2019] and for brass instruments in [Velut et al., 2017] and [Campbell and Bromage, 2005], and was investigated and used to make comparisons between different professional trumpet models in [Fréour et al., 2020]. The purpose of this thesis is to compare the response of different trumpets to varying levels of blowing pressure using numerical continuation methods, as in [Fréour et al., 2020], to make inferences about the instruments that are relevant to players. A small-scale, preliminary perceptual trial was also conducted to determine whether players could perceive these difference and whether they agreed with the conjectures based on the modeling.

1.2 Structure of the Thesis

This thesis begins with a review of brass-instrument modeling techniques in Chapter 2, with a focus on the type of models and analysis used in this thesis. Next, in Chapter 3, the model and methodology used for this thesis are described. The results of the modeling are given in Chapter 4. After the modeling results are presented, the perceptual trial is described, and

its results presented, in Chapter 5. Finally, conclusions are drawn and areas for future work proposed in Chapter 6.

Chapter 2

Brass acoustics modeling background

2.1 Brass Instrument Modeling

2.1.1 Introduction to the trumpet and its sound production mechanism

The trumpet is a member of the brass-instrument family, which consists of instruments whose sound production is facilitated by the musician vibrating, or "buzzing" their lips into a mouthpiece [Campbell et al., 2021]. In the brass-instrument sound production mechanism, the player first generates upstream pressure inside their mouth. The difference between this upstream pressure and the downstream pressure in the mouthpiece generates an airflow that causes the lips to vibrate, and this vibration excites the resonant modes of the instrument. The trumpet itself consists of a cylindro-conical pipe with an exponentially flared bell that resonates at a number of natural frequencies. The player manipulates their blowing pressure and lip position, or "embouchure," so that their lips oscillate inside the mouthpiece at an appropriate frequency to excite a desired resonance mode of the instrument.

2.1.2 Brass instrument modeling approaches

The brass-instrument sound-production mechanism consists of three main components: the lips, which act as the generator of the oscillation, the instrument, which acts as resonator, and the airflow between them. Various studies have investigated the dynamics of the individual components and suggested models for the player-instrument system.

Lip modeling

The first accurate description of the lip-reed system was by von Helmholtz [1954], who classified the direction of vibration into "striking inwards," which describes cases such as a clarinet reed, where the reed or lip reed is blown closed by the player's air pressure, and "striking outwards," where the reed or lip reed is blown open. Later, photographic and videographic methods were used to study the lip motion of brass players in more detail. The first study of this kind was by Martin [1942], who took high-speed photographs of trumpet players' lips while playing on a transparent mouthpiece under stroboscopic light. Martin found that lip vibration occurred both parallel to the direction of airflow, as in Helmholtz's striking-inwards and striking-outwards models, and perpendicular to the airflow, referred to as transverse motion. Martin also found that the displacement of the lip orifice was almost sinusoidal, that the lips closed very briefly once every cycle, and that higher-frequency oscillations had a smaller amplitude of vibration. Further studies by Leno [1971] and Copley and Strong [1996] observed similar phenomena. In a study of lip vibration for trombone players, Copley and Strong found that the lips' motion favoured the longitudinal direction of vibration in the low range, and the transverse direction in the high range. This observation is supported by modeling done by Yoshikawa [1988], Yoshikawa and Plitnik [1993], and Adachi and Sato [1996].

The motion of the lips in these directions has been modeled using one or more springs, as shown in Figure 2.1 from [Adachi and Sato, 1995]. In each case, the difference between the upstream pressure p_0 within the player's mouth and the downstream pressure p in the mouthpiece leads to Bernoulli pressure, which causes airflow through the lips. In the striking-inwards (a) and striking-outwards (b) models, the spring is displaced in the direction parallel to the airflow, while in the transverse direction (c), the spring is displaced in the direction perpendicular to the airflow.

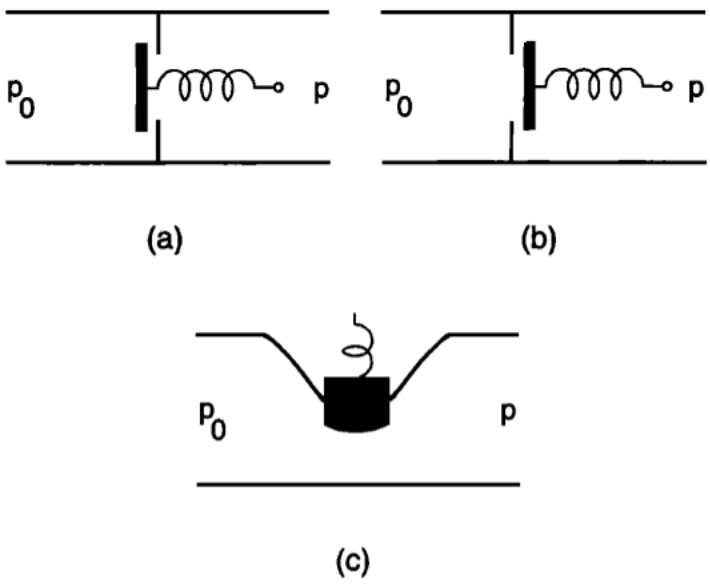

Figure 2.1: Spring orientation for striking inwards (a), striking outwards (b), and transverse (c) models of lip motion, from Figure 1 in [Adachi and Sato, 1995].

Adachi and Sato [1995] propose two models for lip motion, corresponding to the striking-outwards and transverse models. For both of these models, the motion of the upper and lower lips are assumed to be symmetrical. Their striking-outwards model, depicted in Figure 2.2, is described by Equation 2.1,

$$ml\frac{\mathrm{d}^2\theta}{\mathrm{d}t^2} = -\frac{\sqrt{mk}}{Q}l\frac{\mathrm{d}\theta}{\mathrm{d}t} + \frac{1}{2}bl(p_0 - p(t)) + bdp_{lip}\sin(\theta) - kl(\theta - \theta_0), \tag{2.1}$$

where m is the mass of the lips, θ is the lip angle at time t, k is the stiffness of the lips, l is the length of the lips, b is the breadth of the lip orifice, d is the thickness of the lips, p_0 is the upstream blowing pressure, $p(t)$ is the mouthpiece pressure at time t, Q is a lip quality factor, and p_{lip} is the pressure in the lip orifice. The first term on the right-hand side represents the damping force of the spring, the second is the external force due to the pressure difference between the upstream and downstream pressure, the third is the Bernoulli force due to the difference between the mouth pressure and the mouthpiece pressure, and the fourth is the restoring force of the spring.

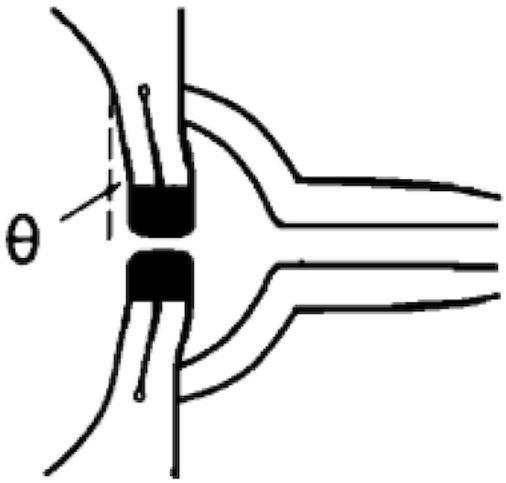

Figure 2.2: Diagram of lip motion in the striking-outwards model from Figure 3(b) in [Adachi and Sato, 1995], where θ is the lip angle at time t.

Adachi and Sato's transverse model, depicted in Figure 2.3, is described by Equation 2.2,

$$m\frac{\mathrm{d}^2y}{\mathrm{d}t^2} = -\frac{\sqrt{mk}}{Q}\frac{dy}{dt} + bdp_{lip} - ky, \tag{2.2}$$

where y is the vertical lip displacement of the upper lip at time t, with the displacement of the lower lip equal to $-y$ due to symmetry, the first right-hand term represents damping force of the spring, the second the Bernoulli pressure, and the third the spring's restoring force. The rest of the parameters are the same as in Equation 2.1. Similar models are used by Fréour et al. [2020] and Rodet and Vergez [1996].

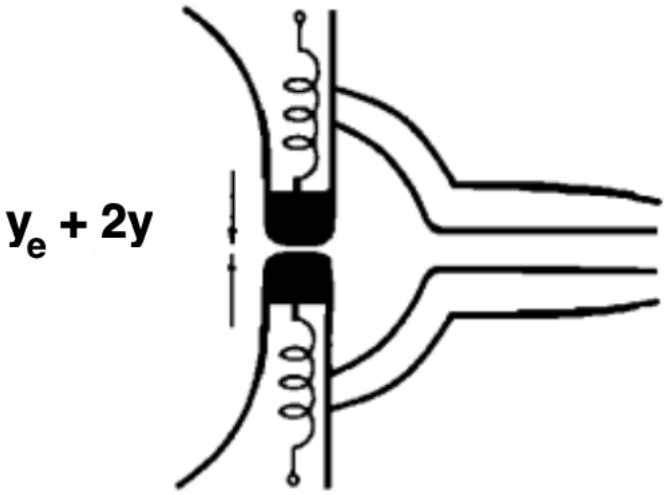

Figure 2.3: Diagram of lip motion in the transverse model from Figure 3(a) in [Adachi and Sato, 1995], where y is the displacement from equilibrium of the upper lip at time t, $-y$ is the displacement of the lower lip at time t, and y_e is the distance between the lips at equilibrium, so that the distance between the lips at time t is equal to $y_e + 2y$.

Adachi and Sato [1996] combine these two equations into one model, where either the striking-outwards or the transverse model is favoured, according to the range in which the performer is playing. Another two-dimensional model describing motion in these two planes is introduced in [Di Federico and Borin, 1997]. Although the stroboscopic measurements

by Martin [1942], experiments carried out by Yoshikawa [1995] and modeling described in [Adachi and Sato, 1996] all suggest that trumpet players' lip motion is in both the transverse and outward-striking directions, and is therefore best described by a model with two degrees of freedom, a one-dimensional model is sufficient for some applications [Velut et al., 2017]. Experimental evidence in [Yoshikawa, 1995] suggests that trumpet tones of the instrument's fourth resonance mode are sustained through transverse oscillation. We only study the fourth mode in this project, and similar studies by Velut et al. [2017] and Fréour et al. [2020] have previously used a one-dimensional transverse model, so a one-dimensional transverse lip model is used for this research.

Airflow modeling

The airflow between the lips and into the instrument is generated by the difference in pressure between the "upstream" region, which includes the mouth cavity and lip orifice, and the "downstream" region inside the mouthpiece. These regions are illustrated in Figure 2.4, from [Velut et al., 2017].

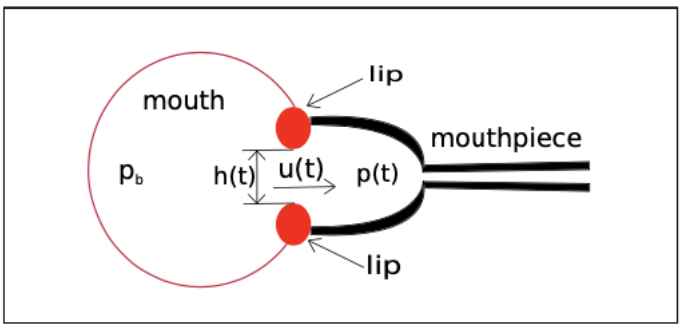

Figure 2.4: Diagram from Figure 2 in [Velut et al., 2017] showing the upstream (mouth) and downstream (mouthpiece) regions, and the flow $u(t)$ between them. The pressure in the upstream region is given by p_b, the pressure in the downstream region is given by $p(t)$, and the height of the lip opening is given by $h(t)$.

The airstream is assumed to be laminar in the upstream region and turbulent in the mouthpiece. Assuming that there is an incompressible, steady flow, and that there is no friction, Bernoulli's equation can be applied. Combining these assumptions with the mass conservation law, the airflow through the lips can be described using Equation 2.3 from [Velut et al., 2017], where $u(t)$ is the volume flow, ρ is the density of air, W is the width of the lip channel, $h(t)$ is the height of the lip channel, p_b is the upstream blowing pressure, and $p(t)$ is the pressure in the mouthpiece.

$$u(t) = \sqrt{\frac{2}{\rho}} W h(t) \sqrt{p_b - p(t)} \tag{2.3}$$

The airflow between the generator and resonator of a player-instrument system for brass instruments is generated by the difference between the "upstream" blowing pressure in the player's mouth, and the "downstream" pressure in the mouthpiece, and is often represented using Bernoulli's equation.

Modeling the resonator

The linear acoustical properties of a resonator can be characterized in terms of its input impedance, which represents the acoustic response of an instrument over a range of frequencies, and can be analyzed to make conjectures about the behaviour of the instrument. In the case of the resonator of a woodwind or brass instrument system, the air inside the air column vibrates as an acoustic system, and the impedance of the system is defined as the ratio of acoustic pressure p to acoustic volume flow U. Given a fixed volume flow, a high acoustical impedance for a given frequency will indicate a high acoustic pressure response is generated, while a low impedance means that a low acoustic pressure response is generated. Since the lip mechanism for brass instruments functions as a

pressure-controlled valve, with the system being mostly closed at the mouthpiece end, a peak in acoustic impedance corresponds to a resonant mode of the instrument [Wolfe]. An impedance measurement represents the instrument's acoustic properties in the frequency-domain, and the impedance can also be converted to an impulse response in the time domain through the inverse Fourier transform, to be used for numerical sound synthesis. The acoustic impedance of a system can be modeled, as in [Adachi and Sato, 1995, 1996], or measured, as in [Fréour et al., 2020].

When a measured impedance is used, the quantity can be fitted to create a representation of the impedance that is more efficient and to smooth out irrelevant noise. Typically, the impedance is parameterized as a sum of complex modes in terms of its poles s_n and modal coefficients, or "residues," c_n, as in Equation 2.4.

$$Z(\omega) = Z_c \sum_{n=1}^{N} \left(\frac{c_n}{j\omega - s_n} + \frac{c_n^*}{j\omega - s_n^*}\right) \tag{2.4}$$

Various fitting schemes have been proposed to extract the parameters c_n and s_n from a measured acoustic impedance. One popular method is the Estimation of Signal Parameters via Rotational Invariance Techniques (ESPRIT), intended for obtaining high-resolution, unbiased estimates of signal parameters in the presence of noise [Roy and Kailath, 1989]. This makes it particularly effective for cases where there is strong overlap between modes [Ablitzer, 2021], and has been used previously for creating a modal fit of a trumpet impedance to be used in a numerical analysis scheme [Fréour et al., 2020]. Maestre et al. [2018] propose a technique that models the acoustic impedance and sound pressure radiation jointly as parallel digital filters. To extract modal parameters from an impedance measurement using the ESPRIT system, the measurement must be converted to a time-domain impulse response, which involves extrapolating the impedance measurement

to 0 Hz, making the impedance hermitian, and applying the inverse Fourier transform. The method in [Maestre et al., 2018] is performed in the z-domain, which is the discrete-time equivalent of the s-domain that is used for the modeling in this thesis. Therefore, the results from the model in [Maestre et al., 2018] would need to be transformed to the s-domain using the bilinear transform before being used in our model. The bilinear transform would also cause frequency warping in the transformation to the z-domain, which would make it not ideal for the purposes of this modeling. The fitting procedure from [Ablitzer, 2021] is applied directly to the measured input impedance, and yields the desired parameters c_n and s_n without transformation, so this is the method selected for this project.

2.2 Hysteresis behaviour

Hysteresis refers to the dependence of a system's state on its history. In the context of brass-instrument system dynamics, this usually refers to the phenomenon that makes it possible to diminuendo, or reduce the playing loudness, to a softer dynamic than it is possible to begin a note. In other words, it is possible to play more softly when reducing the playing dynamic of a note that is already sounding than it is when starting from silence. This phenomenon has been observed in results from previous modeling in [Fréour et al., 2020] and in observations of lip vibration using an artificial mouth and recorded with a high-speed camera in [Campbell and Bromage, 2005].

2.3 Linear Stability Analysis (LSA)

Linear stability analysis (LSA) refers to the process of approximating the dynamics of a nonlinear system around an equilibrium point as a linear system, through linearization. We use a first-order Taylor series to approximate the system's behaviour when we make very small perturbations to the system's state. This type of analysis can be used to either find out how to sustain a system's equilibrium behaviour while slightly varying parameters, or determine how much a parameter needs to be changed to significantly alter the behaviour of a system [Sayama, 2015].

Rodet and Vergez [1996] proved that LSA can be used to determine the minimum blowing pressure required to start a note, and found that their results from LSA were very close to the results obtained through numerical simulation. LSA has since been used to determine factors such as the onset pressure threshold value for a given note on an instrument in [Velut, 2016] and [Velut et al., 2017], as well as the lip parameters that will minimize the onset pressure value in [Fréour et al., 2020].

2.4 Bifurcation analysis

A bifurcation in a nonlinear system of differential equations is a point where a small change in a parameter value leads to a qualitative change in the behaviour of the system's solution. A Hopf bifurcation refers to a critical point for a system where its stability changes and a periodic solution emerges. There are two types of Hopf bifurcation. A supercritical, or direct Hopf bifurcation is a Hopf bifurcation for which the oscillating solution that emerges from the unstable fixed point is quickly stabilized at a low amplitude, i.e. the threshold of extinction for the equilibrium solution is equal to the oscillation threshold. A subcritical, or indirect

Hopf bifurcation is a Hopf bifurcation for which the oscillating solution that emerges from the unstable fixed point immediately jumps to a large amplitude. Identifying the location and type of Hopf biufurcation points for a musical instrument system can give information about how the system's behaviour changes as certain parameters are varied.

Typically, bifurcation diagrams that show the behaviour of the system around a bifurcation point are generated by solving a nonlinear system either theoretically or numerically, to see how one parameter of interest varies with respect to another. One common application of bifurcation analysis is to determine the onset threshold for the beginning of a note locating by the Hopf bifurcation, and to determine the presence and extent of hysteresis behaviour by identifying the type of Hopf bifurcation. Dalmont et al. [2005] use analytical methods to find and classify Hopf bifurcation points for a clarinet model. They find the equilibrium solution that occurs when air is blown into the instrument but no note sounds, and plot the behaviour of the system as the blowing pressure is increased until a Hopf bifurcation occurs and the oscillating solution that corresponds to a note sounding emerges. For their clarinet model, a subcritical Hopf bifurcation was found for the onset of the oscillating solution at all parameter values tested. This means that the player is able to begin a note from essentially silence, and that there is no hysteresis behaviour when they diminuendo to end the note. The extinction threshold for the clarinet model was also examined by creating a bifurcation diagram that showed the blowing pressure at which the oscillating solution ended and a new equilibrium emerged, in order to determine the dynamic range of the instrument. Colinot et al. [2019] examined the oscillation threshold for a conical, saxophone-like instrument modeled as a lossless conical waveguide using numerical continuation methods. They found that the Hopf bifurcation for this model was supercritical for all values of the geometrical

parameters for which they performed their analysis.

For conical brass instruments, the onset threshold can occur at either a subcritical or supercritical Hopf bifurcation, though supercritical is more common. Mattéoli et al. [2021] test the oscillation threshold of a generic brass-type instrument model at various oscillation regimes across its range using numerical continuation methods, and find both supercritical and subcritical Hopf bifurcations depending on the range being tested.

2.5 Numerical continuation methods

2.5.1 Introduction to numerical continuation methods

Another tool for the analysis of acoustic musical instruments that has been applied to brass and woodwind instruments is numerical continuation, or path-following methods. These methods are used to compute approximate solutions to nonlinear systems through parameterization of one variable. Using numerical continuation methods, we can observe the effect of changing one parameter on the behaviour of a system by following solution paths.

The principle of numerical continuation is that, if a stable solution of a system is located, there should be other stable solutions nearby if the system parameters are varied slightly. Consider the following system from [Doedel, 2010]:

$$\mathbf{G}(\mathbf{u}, \lambda) = 0, \qquad u, G(\cdot, \cdot) \in R^n, \lambda \in R \tag{2.5}$$

Let $x \equiv (\mathbf{u}, \lambda)$. Then the equation can be written

$$\mathbf{G}(\mathbf{x}) = 0, \qquad \mathbf{G} : R^{n+1} \mapsto R^n. \tag{2.6}$$

By a theorem proven in [Doedel, 2010], if $x_0 \equiv (\mathbf{u}_0, \lambda_0)$ is a regular solution of $\mathbf{G}(\mathbf{x}) = 0$, then, near $\mathbf{x}_0$, there exists a unique one-dimensional continuum of solutions

$$\mathbf{x}(s), \text{ with } \mathbf{x}(0) = \mathbf{x}_0. \tag{2.7}$$

In other words, in the region near a regular solution of a system, we can follow a path of solutions, beginning with this solution, by varying one of the system parameters. This principle can be applied to determine the effect of varying one parameter on the overall behaviour of a system, and has been applied towards the classification of musical instruments.

2.5.2 Use of numerical continuation methods to classify acoustic instruments

Karkar [2012] and Fréour et al. [2020] use numerical continuation methods to create bifurcation diagrams of system solutions for woodwind and brass instruments, respectively, using measured acoustic impedances, and relate these bifurcation diagrams to instrument attributes that are relevant to players. Karkar [2012] uses a numerical continuation approach to investigate the effect of various parameter values on the oscillation threshold for single reed instruments. The instrument is considered as a dynamical system, and the problem is approached through continuation of periodic solutions at Hopf bifurcations. Fréour et al. [2020] apply these techniques specifically to trumpets by first developing modal representations of measured trumpet impedances using the high-resolution subspace method: Estimation of Signal Parameters via Rotational Invariance Techniques (ESPRIT)

[Roy and Kailath, 1989]. They then use numerical continuation to follow the paths of periodic solutions of coupled system equations to generate bifurcation diagrams and identify the Hopf bifurcations and other landmarks of the system for solutions corresponding to a $B_4^\flat$ on each trumpet. The locations of these landmarks are compared between instruments and used to define two quantities for a given instrument: the "amplitude of the hysteresis," related to the differences between onset and offset pressures for the mouth and for internal acoustic pressure, and the "dynamic range," which represents how much the sound pressure can vary when the player uses a blowing pressure of up to 5 kPa.

2.5.3 Manlab

Manlab is a Matlab package, developed at the Laboratoire de Mécanique et d'Acoustique in Marseille, France, a unit of the Centre National de la Recherche Scientifique (CNRS). It uses the asymptotic numerical method (MAN) algorithm, described in [Cochelin et al., 2007], to solve systems of the form

$$\mathbf{R}(\mathbf{U}) = 0, \tag{2.8}$$

with $\mathbf{R}$ a vector of n smooth equations, and $\mathbf{U}$ a vector of $n+1$ unknowns [Lejeunes, 2011]. Manlab 4.1.5 was downloaded from [Lejeunes, 2011] and used to perform the numerical continuation used in this thesis.

Chapter 3

Methodology

The methodology used in this thesis involves first deriving a physical-equation model of the trumpet-player system that uses a modal representation of a measured impedance to characterize the resonance of each trumpet. The model is then analyzed for each trumpet using numerical continuation methods to make inferences about characteristics such as the minimum blowing pressure required to start a note on the instrument, its hysteresis behaviour, and the dynamic level of the sound produced at various levels of blowing pressure.

Examples of the Manlab files used for the numerical continuation in this thesis can be found in [Hopkins, 2023].

3.1 Impedance representations

The acoustic impedances of four trumpets with open fingering (no valves pressed) were measured using the CapteurZ system, described in [Le Roux, 2013]. The trumpets measured are a Yamaha model YTR-8335RS25TH, a Vincent Bach Stradivarius model 37,

Manufacturer	Model	Abbreviation
Yamaha	YTR-8335RS25TH (Xeno 25^{th} Anniversary limited Model)	Y
Bach	Stradivarius Model 37	S1
Bach	Stradivarius Model 37 with modified leadpipe by Savût Trumpets	S2
Besson	Unknown (vintage student model)	B

Table 3.1: Trumpets used for the project.

a Vincent Bach Stradivarius model 37 with its lead pipe modified by Savût Trumpets to allow for an adjustable annulus gap size, and a Besson trumpet of an unknown model. The first three trumpets are professional model instruments, and the last is a student model. These instruments were chosen to provide an opportunity for comparison between two of the most popular professional trumpet manufacturers, between professional and student model instruments, and between two trumpets of the same make and model with and without post-manufacture modifications. Though the sample size will not be large enough to draw conclusions about any of these factors, interesting hypotheses may be made about their influence on the results. Additionally, anecdotal evidence from trumpet players suggest that there are perceptible differences between these instruments that make them feel different from one another to play. Going forward, these instruments will be referred to as Trumpets Y, S1, S2, and B, with Y being the Yamaha instrument, S1 the unmodified Bach Stradivarius, S2 the modified Bach Stradivarius, and B the Besson. The trumpets used for this project are summarized in Table 3.1.

The impedances of these trumpets were measured using a sine sweep from 100 to 6000 Hz, which includes the second through eighth impedance peaks for each trumpet, which is sufficient for studying the fourth resonance of each. Modal representations of each of

the measured impedances were then determined using code from [Ablitzer, 2022], based on Ablitzer [2021]. The fitting procedure yields the variables ξ_n, ω_n, A_n, and B_n, which can be used to determine the poles s_n and residues C_n in Equation 2.4 using Equations 3.1 and 3.2. These modal parameters are used to represent the impedance for each trumpet in the trumpet-player system model.

$$s_n = -\xi_n\omega_n + j * \omega_n\sqrt{1-\xi_n^2} \tag{3.1}$$

$$\begin{cases} \Re(c_n) = \frac{A_n}{2} \\ \Im(c_n) = \frac{1}{2}\frac{\xi_n\omega_n A_n - B_n}{\omega_n\sqrt{1-\xi_n^2}} \end{cases} \tag{3.2}$$

3.2 Model description

The model used for this research was used in [Fréour et al., 2020] and [Velut et al., 2017], and is based on previous models such as the transverse model in [Adachi and Sato, 1995]. It consists of equations representing three parts: the motion of the lips, the response of the instrument, and the airflow between the two.

The lip motion is modeled as one-dimensional motion in the direction perpendicular to the airflow, referred to as the transverse model previously. The model is also a "blown open" model, meaning that the difference between the air pressure inside the player's mouth and inside the mouthpiece causes the lips to open. Though Velut et al. [2017] refer to this as a "striking outwards" model, it is important to note that the direction of motion does not correspond to that of the "striking outwards" model in [Adachi and Sato, 1995], but rather the transverse direction. The lip equation is given by

$$\ddot{y} + \frac{\omega_l}{Q_l}\dot{y} + \omega_l^2(y - y_0) = \frac{p_0 - p(t)}{\mu_l}, \tag{3.3}$$

where y is the vertical lip position at time t, ω_l is the resonance frequency of the lips, Q_l is the quality factor of the lips, y_0 is the lip position at rest, p_0 is the blowing pressure inside the player's mouth, $p(t)$ is the pressure inside the mouthpiece at time t, and μ_l is the lip mass per unit surface area.

The airflow through the lips is given by Bernoulli's equation with conservation of mass, assuming that the flow is laminar in the mouth and turbulent in the mouthpiece. The equation of the airflow is given by

$$u(t) = \sqrt{\frac{2|p_0 - p(t)|}{\rho}} b \cdot \text{sign}(p_0 - p(t)) \cdot y(t) H(y(t)), \tag{3.4}$$

where $u(t)$ is the volume flow through the lip opening, ρ is the density of air in kgm^{-3}, b is the breadth of the lips, and H is the Heaviside function, forcing the flow to zero when the lips are closed.

Finally, the response of the instrument is taken from the modal representation of its input impedance. Recall that the modal representation is given by 2.4, in terms of its complex poles s_n and residues C_n. As in [Fréour et al., 2020] and [Velut et al., 2017], the complex pressure component for a mode n is given by

$$P_n(\omega) = Z_c \frac{C_n}{j\omega - s_n} U(\omega), \tag{3.5}$$

so that in the time domain, we have

$$\dot{p}_n(t) = Z_c C_n u(t) + s_n p_n(t). \tag{3.6}$$

Silva [2009] shows that the pressure in the mouthpiece $p(t)$ can be derived from the pressure components as follows:

$$p(t) = 2 \sum_{n=1}^{N} \Re(p_n(t)). \tag{3.7}$$

The overall system used is then the combination of equations 3.3 and 3.6, with the volume flow $u(t)$ given by 3.4, and the mouthpiece pressure given by 3.7. The real and complex pressure components are calculated separately, giving the system in 3.8, referred to as System A in this thesis.

$$\begin{cases} \ddot{y} + \frac{\omega_l}{Q_l}\dot{y} + \omega_l^2(y - y_0) = \frac{p_0 - p(t)}{\mu_l}, \\ \dot{R}_n = \Re(\dot{p}_n(t)) = \Re(Z_c C_n u(t) + s_n p_n(t)), \forall n \in [1, N], \\ \dot{I}_n = \Im(\dot{p}_n(t)) = \Im(Z_c C_n u(t) + s_n p_n(t)), \forall n \in [1, N], \end{cases} \tag{3.8}$$

where N is the number of modes fitted in Section 3.1.

The lip parameter values used are the same as those used in [Fréour et al., 2020], aside from the lip natural frequency, which is obtained through linear stability analysis in the next section, and the lip quality factor, which was adjusted slightly and set to $Q = 3.2$ in order to excite the desired resonance on all four trumpets. This value is still well within the range found by Velut et al. [2017] in his review of lip parameter values from eight different studies.

3.3 Linear Stability Analysis to determine lip parameters

Before analysing System A, LSA is used to determine the best natural lip frequency with which to excite the system. Trumpet players control their natural lip frequency using their embouchure, and in [Fréour et al., 2020], it is assumed that players position their embouchure in order to minimize the blowing pressure required to start a note. Though a player may modify their embouchure based on many factors for a single note, including dynamics, articulation, and tone quality, for this thesis, the lip resonance frequency alone will be optimized to minimize the blowing pressure required to start a note, instead of adjusting all factors simultaneously. This simplification is based on the assumption that the complex and interconnected adjustments made by a player can be approximated by modifying the natural lip frequency alone.

To use LSA, an equilibrium solution for System A is first obtained by setting all time derivatives to zero. This equilibrium point corresponds to the state where the player is blowing into the instrument, but not with sufficient blowing pressure to excite an oscillation. The variables $y(t)$ and $p(t)$ are notated as y_e and p_e at equilibrium, and the n^{th} component of $p(t)$ is notated as p_{ne} at equilibrium.

$$\begin{cases} 0 = -\omega_l^2 y_e - \frac{p_e}{\mu_l} + \omega_l^2 y_0 + \frac{p_0}{\mu_l} \\ 0 = s_n p_{ne} + Z_c C_n \sqrt{\frac{2}{\rho}} b y_e \sqrt{p_0 - p_e} \\ u_e = \sqrt{\frac{2}{\rho}} b y_e \sqrt{p_0 - p_e} \end{cases} \tag{3.9}$$

Next, the Jacobian matrix of System A is computed. Following the derivation from [Velut, 2016], let $C = \sqrt{p_0 - p_e}$ and recall the modal representation of $Z(\omega)$ given in 2.4.

Considering the relationship between $p(t)$ and $p_n(t)$, the real parts of both sides of the third system equation and can be summed and multiplied by two, the value of $Z(\omega = 0)$ can be substituted, which gives Equation 3.10:

$$\begin{cases} y_e = y_0 + \frac{C^2}{\mu_l \omega_l^2} \\ u_e = \sqrt{\frac{2}{\rho}} b y_e C \\ p_e = Z(\omega = 0) u_e. \end{cases} \tag{3.10}$$

Equation 3.10 can be combined into one line, as in 3.11.

$$\frac{bZ(\omega = 0)}{\mu_l \omega_l^2} \sqrt{\frac{2}{\rho}} C^3 + C^2 + b y_0 Z(\omega = 0) \sqrt{\frac{2}{\rho}} C - p_0 = 0 \tag{3.11}$$

Now that the equilibrium solution has been determined, the solution to System A can be approximated in nearby regions using a Taylor series approximation for functions of many variables. A first-degree version of this approximation is given by

$$F(X) = F(X_e) + J(X_e) * (X - X_e), \tag{3.12}$$

where X_e is an equilibrium point of System A, $J(X_e)$ is the Jacobian matrix of System A, and X is a point near the equilibrium, with one or more of the system parameters changed by a small amount. The Jacobian matrix of System A is defined as

$$J(X) = \begin{bmatrix} \frac{\partial f_1}{\partial x_1} & \cdots & \frac{\partial f_1}{\partial x_n} \\ \vdots & \ddots & \vdots \\ \frac{\partial f_n}{\partial x_1} & \cdots & \frac{\partial f_n}{\partial x_n} \end{bmatrix} \tag{3.13}$$

See [Velut, 2016] for a full derivation and statement of the Jacobian matrix for System

A. The solution to $\dot{X} = F(X)$, with $F(X)$ as defined in 3.12 is given by

$$X(t) - X(e) = \sum_{i=1}^{N} U_i e^{\lambda_i t}, \tag{3.14}$$

where λ_i are the eigenvalues of the matrix $J(X)$, and U_i are the corresponding eigenvectors. If any of the eigenvalues has a positive real part, the solution will tend to infinity as time increases, and therefore be unstable [Sayama, 2015]. The point where this solution becomes unstable corresponds to a Hopf bifurcation point, from which the oscillating solution corresponding to a periodic sounding tone emerges.

To find the lip frequency value ω_l for which the blowing pressure p_0 required to start the note is minimized, an array of possible ω_l values around the expected frequency region required to excite the fourth resonance on the trumpet are chosen, and for each one, the eigenvalues of the Jacobian matrix for increasing values of p_0 are calculated. For each ω_l value, as soon as the matrix has a positive eigenvalue, the p_0 value is recorded. Once the threshold p_0 values have been found for all chosen values of ω_l, the minimum recorded p_0 threshold value is found, and the corresponding ω_l value is selected as the natural lip frequency for the instrument. A plot of the p_0 value at the minimum onset threshold vs. $f_{lip} = \frac{\omega_l}{2\pi}$ is given in 3.1.

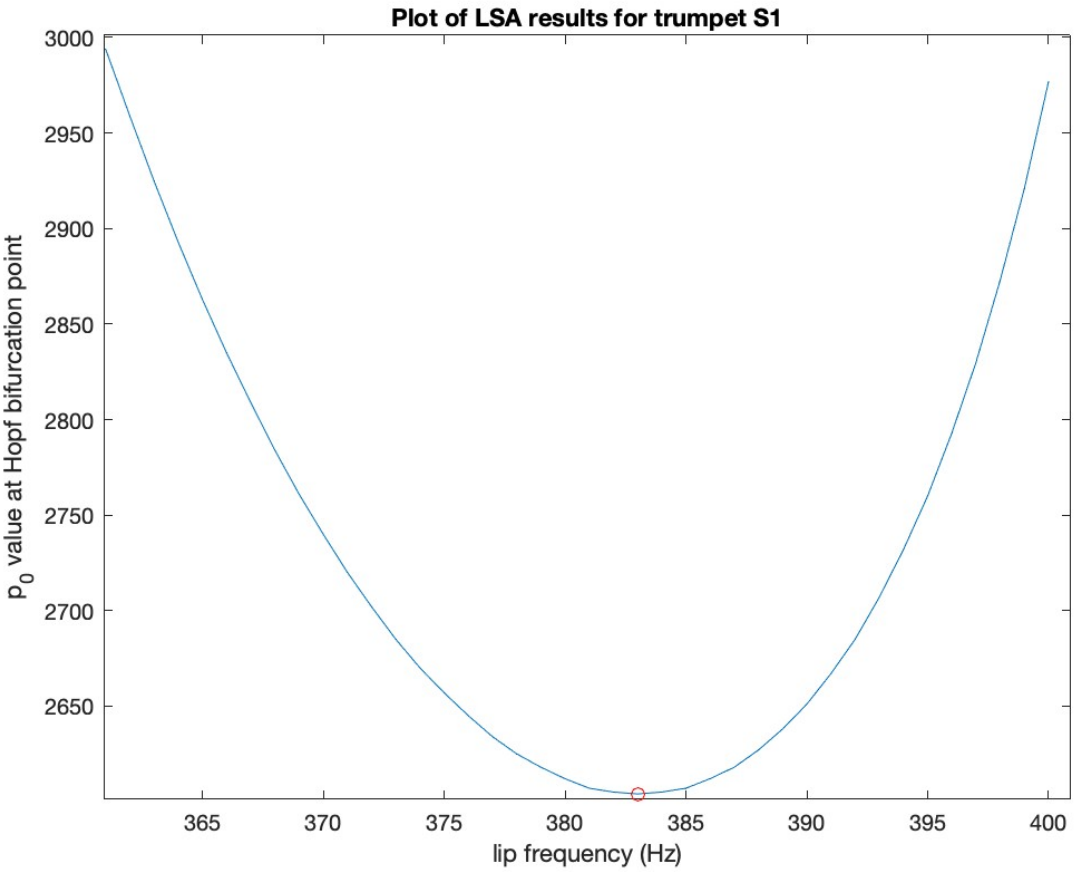

Figure 3.1: Plot of minimum onset pressure vs. lip frequency for Trumpet S1. The minimum, marked with a red circle, shows the value chosen for f_{lip} for this instrument.

A summary of the ω_l values, with the corresponding lip frequency and p_0 threshold values, is in Table 3.2.

3.4 Numerical continuation

We use numerical continuation to follow the behaviour of the solution as one parameter is varied. The Manlab software allows us to plot the value of one system parameter against

Trumpet	$\omega_l = 2\pi f_{lip}$	f_{lip} (Hz)	p_0 threshold value (Pa)
Trumpet Y	2424.3	385.84	2088.0
Trumpet S1	2409.3	383.45	2613.4
Trumpet S2	2429.8	386.71	2165.7
Trumpet B	2304.8	366.82	4626.9

Table 3.2: Summary of LSA results.

another for a given system solution to see the effect of varying one parameter. For this project, we vary the player's blowing pressure p_0 and plot it against the pressure inside the mouthpiece, p.

Before we use Manlab for numerical continuation, we must modify System A so that the vector equation is written as a polynomial with quadratic nonlinearity, of the form

$$R(U) = L0 + L(U) + Q(U, U) = 0, \tag{3.15}$$

where $L0$ is a constant vector, L is a linear operator with respect to U, and Q is a bilinear operator with respect to U [Karkar et al., 2011]. For this research, a quadratic form of System A is used, derived by Fréour et al. [2020]. This new system, referred to in this thesis as System B, uses dimensionless variables derived from its system variables, which are given in Equation 3.16.

$$
\begin{cases}
x = \frac{y}{y_0}, \\
P_M = \mu_l \omega_l^2 y_0, \\
\lambda = \frac{p_0}{P_M}, \\
\tilde{p} = \frac{p}{P_M}, \\
\tilde{R}_k = \frac{R_k}{P_M}, \\
\tilde{I}_k = \frac{I_k}{P_M}, \\
\tilde{u} = u\frac{Z_c}{P_M}, \\
\tilde{v} = \frac{v}{\sqrt{2P_M/\rho}}, \\
\xi = Z_c b y_0 \sqrt{\frac{2}{\rho P_M}}, \\
\tilde{t} = t\Im(s_1), \\
\tilde{\omega}_l = \frac{\omega_l}{\Im(s_1)}, \\
\tilde{C}_n = \frac{C_n}{\Im(s_1)}, \\
\tilde{s}_n = \frac{s_n}{\Im(s_1)}
\end{cases}
\tag{3.16}
$$

System B has four main variables in quadratic form, given in Equation 3.17, and five auxiliary variables, with corresponding equations given in Equation 3.18:

$$
\begin{cases}
\tilde{\dot{R}}_k = \Re(\tilde{C}_k)\tilde{u} + \Re(\tilde{s}_k)\tilde{R}_k - \Im(\tilde{s}_k)\tilde{I}_k, \\
\tilde{\dot{I}}_k = \Im(\tilde{C})\tilde{u} + \Im(\tilde{s}_k)\tilde{I}_k, \\
\tilde{\dot{x}} = \tilde{\omega}_l \tilde{z}, \\
\tilde{\dot{z}} = \tilde{\omega}_l(1 - x - \frac{1}{Q_l}\tilde{z} + \lambda - \tilde{p}).
\end{cases}
\tag{3.17}
$$

$$\begin{cases} 0 = 2\sum_{k=1}^{N} \tilde{R}_k - \tilde{p}, \\ 0 = x^2 + \epsilon_x - s^2, \\ 0 = \lambda - \tilde{p} - \tilde{v}w, \\ 0 = \tilde{v}^2 + \epsilon_v - w^2, \\ 0 = \xi \frac{(s+x)}{2} \tilde{v} - \tilde{u} \end{cases} \tag{3.18}$$

Equations 3.17 and 3.18 form System B, the system that is implemented in Manlab.

3.4.1 Numerical continuation in Manlab

Manlab is first used to locate the bifurcation detected using LSA in Section 3.3. The software is run with all time derivatives set to zero, with initial conditions corresponding to the equilibrium solution where the player's lips are at rest and their lips are not vibrating. The Manlab GUI is then used to increase the dimensionless blowing pressure parameter λ slowly until the solution becomes unstable, indicating that a Hopf bifurcation has been reached. An example is shown in Figure 3.2, with the stable solution in solid, the unstable solution a dotted line, and the Hopf bifurcation marked with a star.

Once the bifurcation has been located, the state of System B is exported at the bifurcation point using the Manlab GUI and used as input to System B in a new continuation file, now with the time derivatives included. This represents the periodic solution of System B that emerges once the lips begin to oscillate and a sound is produced. The file is run to begin continuation with Manlab's correction feature disabled so that the solution does not correct to the equilibrium solution, then the full continuation diagram is computed to show the behaviour of the downstream pressure parameter $\tilde{p}$ as the blowing pressure λ is varied across

the relevant range of values.

Once continuation plots have been generated for the oscillating solution, the points of interest are identified for analysis. The first point identified is the minimum-blowing-pressure oscillation threshold, which is the blowing pressure value at which the equilibrium solution becomes unstable when the blowing pressure is increased gradually. The amplitude of the mouthpiece pressure at this point is also notated. Next, the location of the fold is determined, or the point at which the oscillating solution loses stability when the blowing pressure is gradually decreased. Finally, the amplitude of the mouthpiece pressure at a blowing pressure of 5 kPa is located, representing an estimate of the mouthpiece pressure produced given the maximum blowing pressure possible for a player. The dynamic range, or the difference in mouthpiece pressure between the 5 kPa reference and the fold, and the amplitude of the hysteresis, or the difference in blowing pressure between the minimum-pressure onset and the fold, are both calculated from these results. These locations can be linked to qualitative traits about each trumpet, and qualified as more or less desirable. It could be expected that the instrument that is most desirable for a player is the instrument that requires the least blowing pressure to start a note, has the lowest minimum dynamic and the highest maximum dynamic, and has the lowest hysteresis amplitude, though discussion with players would be needed to confirm this hypothesis.

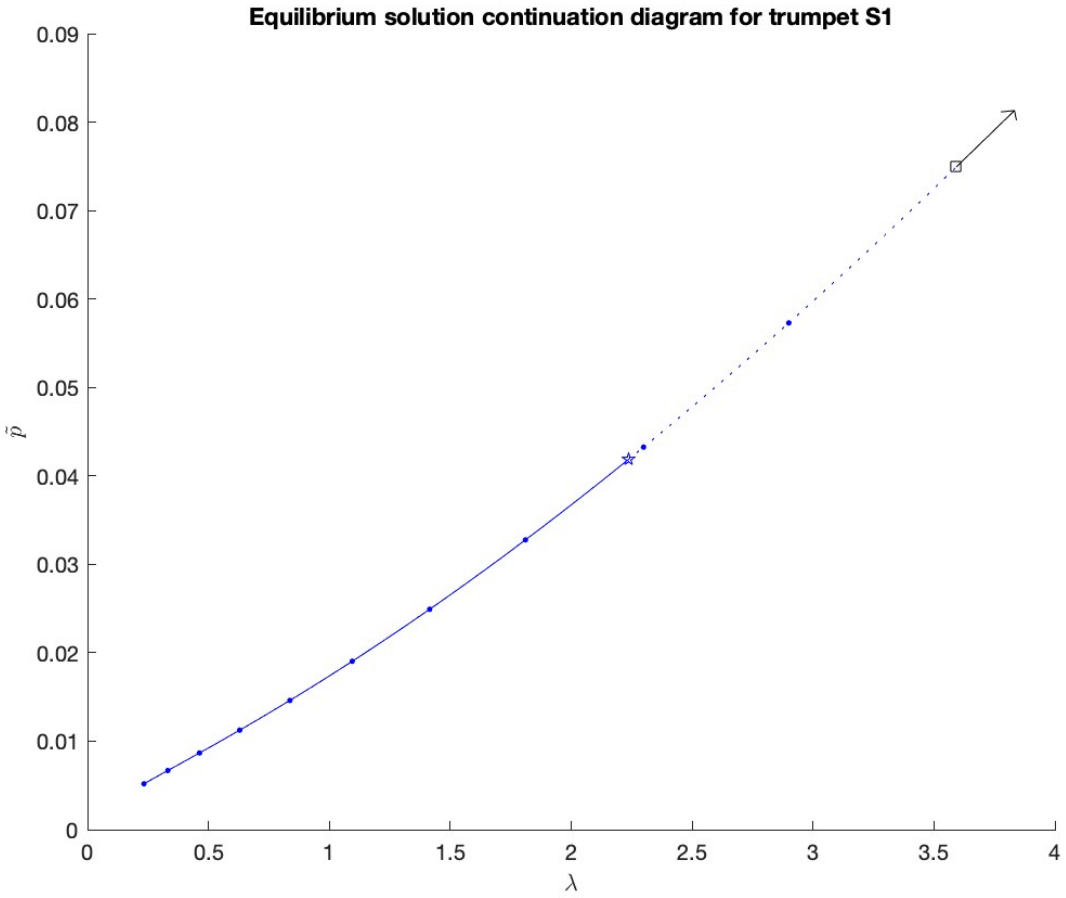

Figure 3.2: Continuation diagram from Manlab of dimenesionless downstream pressure $\tilde{p}$ vs. dimensionless upstream pressure λ, showing the equilibrium solution's transition from stable (solid line) to unstable (dotted line) at the Hopf bifurcation point (starred).

Chapter 4

Results and analysis

Continuation plots were generated for all of the trumpets, as described in Section 3.4.1. The parameters were transformed from their dimensionless form to the upstream and downstream pressure parameters, p and p_0, respectively. Figure 4.1 shows the continuation diagrams for all four trumpets, with the points of interest marked.

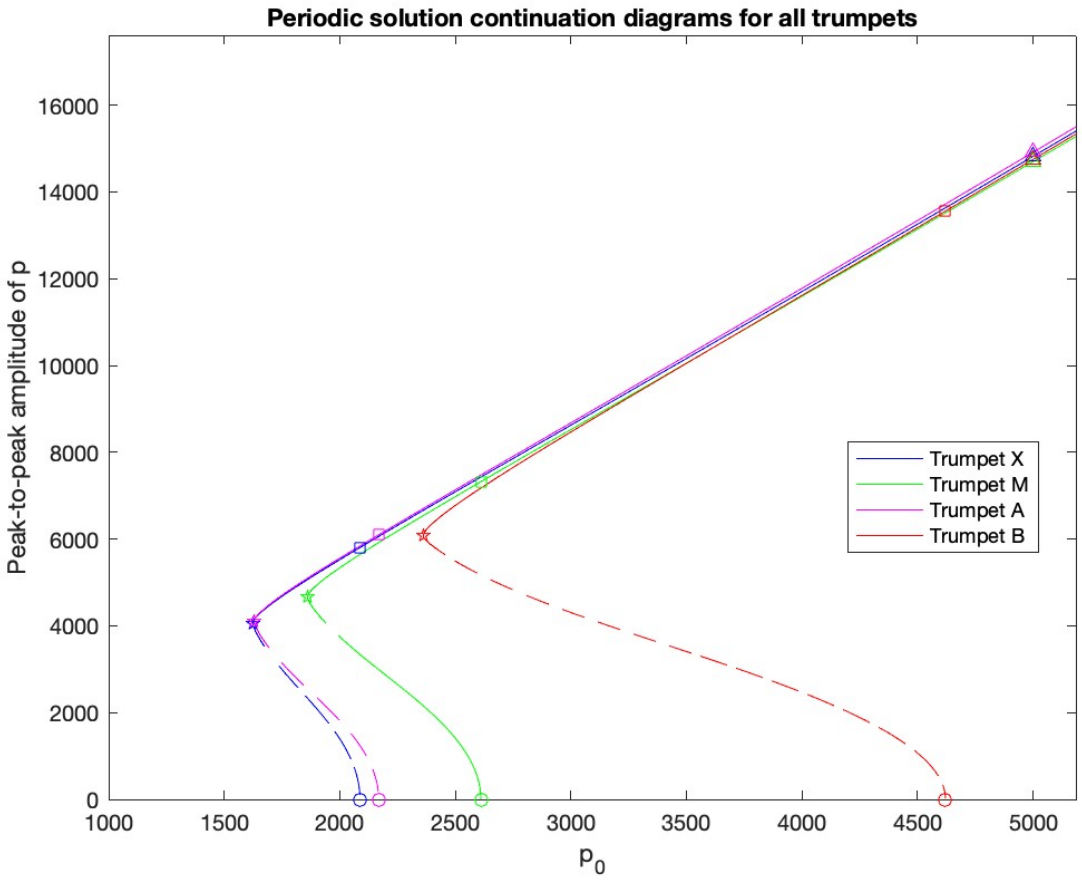

Figure 4.1: Continuation plot for the oscillating solutions for the four trumpets. The Hopf bifurcation points are marked with circles, the amplitude of p at the Hopf points with squares, the folds with a stars, and the values of p at the 5 kPa reference value with triangles. The stable sections of the solutions are plotted with solid lines, and the unstable with dashed lines.

For each instrument, the continuation diagram shows a subcritical Hopf bifurcation point, which means that there is an immediate jump to a large amplitude when the solution emerges. The Hopf bifurcation point, marked with a circle, represents the point at which the equilibrium solution loses stability and the periodic oscillating solution emerges.

This is the point at which, if the player were slowly increasing their blowing pressure from zero, a note would begin to sound. The square marks the p value to which the oscillating solution jumps when it becomes stable, i.e., the downstream pressure level at which the note would begin when started at the minimum oscillation threshold, which is related to the loudness of the sound at its onset.

The continuation diagrams for all of the instruments display hysteresis behaviour. When the solution is continued backwards, decreasing the p_0 value past the Hopf point, it remains stable beyond the Hopf point so the solution is stable for values of p_0 and p lower than the values at the Hopf point, up to the location of the fold, where the solution becomes unstable. The location of the fold is correlated to the point at which the note stops sounding when a player performs a gradual diminuendo beyond their minimum onset pressure.

Finally, when the blowing pressure is continued in the positive direction, the diagram shows how the downstream pressure behaves as the blowing pressure increases. A reference point is marked for p when $p_0 = 5$ kPa for all of the instruments, which is related to the loudness of the sound produced at a reasonable estimate of a player's maximum blowing pressure.

The locations of these points of interest are shown for comparison in Table 4.1.

Trumpet	Hopf bifurcation point (p_0, p) (Pa)	Fold (p_0, p) (Pa)	p value at $p_0 = 5$ kPa (Pa)	Amplitude of hysteresis (distance in p_0 between fold and bifurcation	Dynamic range (difference in p between fold and 5 kPa reference
Y	(2087.5, 5803.7)	(1624.0, 4053.9)	14818.4	463.5	10 764.5
S1	(2610.6, 7320.9)	(1859.8, 4653.8)	14696.6	750.8	10 042.8
S2	(2168.3, 6097.0)	(1629.7, 4095.9)	14912.0	538.6	10 816.1
B	(4621.1, 13558.7)	(2361.4, 6072.4)	14749.0	2259.7	8676.6

Table 4.1: Summary of results of numerical continuation.

The locations of these points of interest can be compared for the different instruments, and conjectures can be made about how the instruments will respond when played by a performer.

First, the location of the Hopf bifurcation can be compared for each instrument. The p_0 value is lowest for Trumpet Y, followed by Trumpets S2, S1, and B. The values are very close together for Trumpets Y and S2, and S1 is fairly close as well, but the p_0 value for Trumpet B is more than 2 kPa above the value for Trumpet S2. Comparing the p values at the Hopf

bifurcation point gives a very similar result: the note begins at the lowest amplitude for Trumpet Y, followed closely by Trumpet S2 and then Trumpet S1, and then Trumpet B at a much higher value. This implies that, if a player used the minimum required onset pressure, they could start playing a $B_4^\flat$ with the least amount of blowing pressure and at the quietest dynamic on Trumpet Y, followed closely by Trumpet S2 at a slightly higher blowing pressure and onset dynamic, then Trumpet S1 a little bit higher for both values, and then Trumpet B, with a much higher blowing pressure and a much louder dynamic. The location of the Hopf bifurcation value for Trumpet B in particular occurs at approximately double the values for the other trumpets, and is very close to the maximum blowing pressure of 5 kPa. As a result, the amplitude of p for the the minimum-pressure-onset note is very close to the maximum amplitude of p for the instrument. This is not consistent with any observations from players or from observing the trial described in Chapter 5, which may mean that the lip parameters chosen are not realistic for Trumpet B.

Next, the location of the fold, where the solution becomes unstable when we continue the solution backwards from the Hopf point, can be observed. This represents the point where the note is extinguished when the player diminuendos to silence. The p value at this point corresponds to the quietest dynamic that can be played on the instrument with the lip parameters as chosen. The same pattern that was noticed for the Hopf point emerges: Trumpet Y has the lowest p and p_0 values at the fold, followed very closely by Trumpet S2 and then Trumpet S1, and Trumpet B has the largest values for both parameters, though the difference is not as large as for the Hopf point. This implies that Trumpet Y can diminuendo to the quietest dynamic and its sound is extinguished at the lowest blowing pressure of the four instruments, with Trumpets S2 and S1 close behind, and that the note is extinguished at the highest blowing pressure and at the least quiet extinction dynamic on Trumpet B. This is

related to the amplitude of the hysteresis, which described the difference in blowing pressure between the Hopf point and the fold, or the amount that the blowing pressure can be reduced beyond the Hopf point before the note is extinguished. For the hysteresis amplitude, the same pattern observed for the Hopf point and the fold emerges: Trumpet Y has the smallest hysteresis amplitude, followed by Trumpet S2, then Trumpet S1, and Trumpet B, with a much larger gap between the hysteresis amplitudes of Trumpet S1 and Trumpet B than for any of the gaps between the values for the first three instruments, implying that for the three professional model trumpets, their minimum volume is relatively close to their onset volume, and that for Trumpet B, the only student-model instrument, the gap is much larger.

Finally, the p value at maximum blowing pressure and dynamic range of the instruments can be examined. The p values at $p_0 = 5$ kPa blowing pressure are all very similar. The value for Trumpet B is the lowest, followed by Trumpet Y, then Trumpet S2, then Trumpet S1, but the differences are all very close, implying that all four trumpets have very similar maximum dynamics. Since the maximum dynamics are similar, the dynamic range correlates closely with the location of the fold. Trumpet B has the smallest dynamic range, followed by Trumpets S1, Y, and S2. Once again, the difference is largest between Trumpet B and the rest of the trumpets.

Chapter 5

Perceptual trial

5.1 Perceptual trial methodology

After the numerical analysis was completed, a small-scale perceptual trial was conducted to see if the features found through modeling could be easily distinguished by experienced trumpet players.[1] Five trumpet players were recruited to participate in the study: four upper-year undergraduate trumpet performance students and one doctoral trumpet performance student. The experiment was conducted in lab A-818 at the Centre for Interdisciplinary Research in Music Media and Technology (CIRMMT), a room free of any strong resonances with surface area of 27m^2 and a reverberation time of approximately 0.18s. Throughout the experiment, the participants wore sunglasses, with the lights of the room dimmed so that they could see the instruments enough to pick them up and play them, but they could not tell them apart visually. The first- and third-valve slides were removed from each instrument, participants were instructed to not move the valves, and

[1] This perceptual trial was carried out under an approved ethics certificate, with Research Ethics Board file number 430-0415.

they were told to only play a concert $B_4^\flat$ so that they could not make assumptions about the instruments based on any factor outside of the scope of the perceptual study, such as the ease of moving the valves and slides or the consistency of tuning across the range of the instrument.

The performers sat in the same position throughout the experiment, with a table in front of them holding the four trumpets. The players were asked to perform five tasks, and for each, they were allowed to pick up the instruments themselves and play the required exercises, repeating the exercises and switching back and forth between the instruments as needed. After playing each exercise, each player placed the instruments in order on the table according to their response.

The tasks and questions asked of the players were as follows. Each question is designed to allow for qualitative comparison between the players' responses and the modeling results.

1. For each instrument, play an air attack as softly and gradually as possible, starting with a blowing pressure too low to cause a note to sound, and increasing the blowing pressure until the note ($B_4^\flat$) sounds. Place the instruments in order from the least blowing pressure required to begin a note to the most.

This task is to assess the player's perception of each instrument's minimum onset pressure, which corresponds to the p_0 value at the bifurcation.

2. For each instrument, perform the same type of air attack as indicated in Task 1, but when the note begins to sound, immediately diminuendo as much as possible until the note is extinguished. Place the trumpets in order from the instrument on which you could diminuendo the least to the one on which you could diminuendo the most.

This task assesses the player's perception of the difference between the onset pressure

and the minimum blowing pressure at which the note can sound (i.e. the blowing pressure at which the note stops sounding as the player gradually decreases their blowing pressure), which corresponds to the amplitude of the hysteresis for each instrument.

3. Once again beginning with a soft air attack, crescendo gradually to your maximum volume. Place the instruments in order from the instrument that requires the least blowing pressure to play at your loudest dynamic to the one that requires the most.

This question does not correspond directly to one of the quantities observed, but is related to the mouthpiece pressure p value at high values of blowing pressure p_0. In this question and the subsequent ones, volume refers to the perceived loudness. The term ”volume“ is used instead of ”pressure“ or “loudness,” even though it corresponds to the amplitude of the mouthpiece pressure, to make the question clear to the performers, who are more familiar with this terminology. This question was included to provide more information about the instrument's response at high blowing pressure and loud dynamics, as it is impossible for players to quantify their exact blowing pressure, which varies from player to player and across repetitions.

4. Repeat the same exercise as in Task 1, but now place the instruments in order from the instrument on which your minimum onset volume is the softest to the one on which the minimum onset volume is the least soft.

This question assesses the minimum onset loudness instead of minimum onset blowing pressure for each instrument, and corresponds to the value of p at the bifurcation.

5. Repeat the same exercise as in Task 3, but now place the instruments in order from the one on which your maximum volume was the least loud to the one on which your maximum volume was the most loud.

This question is to assess the maximum loudness achieved by the player at their maximum blowing pressure, to be compared with the modeled quantity of mouthpiece pressure p at the 5 kPa reference value for p_0, though the player's actual blowing pressure is not controlled or measured.

5.2 Perceptual trial results and analysis

Analysis of variance (ANOVA) testing was carried out on the results for each task, after confirming the assumptions of ANOVA testing using a Durbin Watson test, a Shapiro test, and a Levene test. For all questions, it was found that the trumpet used was not a significant or near-significant factor for determining the ranking, so the test results were not statistically significant for any of the tasks. The results of the trial are summarized below for discussion, and players' comments about the instruments and tests are also discussed.

For each question, the ranking given to each instrument by each participant, the mean ranking and standard deviation for each instrument, and the result we would expect based on the modeling results in Table 4.1 where applicable are summarized.

The results for Task 1 of the perceptual trial are in Table 5.1.

Participant	Trumpet Y ranking	Trumpet S1 ranking	Trumpet S2 ranking	Trumpet B ranking
1	1	2	3	4
2	4	3	2	1
3	2	3	1	4
4	1	4	2	3
5	3	4	2	1
Mean	2.2	3.2	2	2.6
Standard deviation	1.3	0.84	0.71	1.52
Expected from modeling	1	3	2	4

Table 5.1: Results for Task 1 of the perceptual trial. Each instrument is ranked by each player in order from the least blowing pressure required to begin a note (1) to the most (4).

The average rankings for the instruments are all between 2 and 3.2, which are all very moderate rankings, and the rankings do not seem to correlate with the expected rankings from the modeling. There is also a lot of variation between the players' rankings for each instrument, implying that the players did not agree amongst themselves.

We find similar observations for the second, third, fourth, and fifth tasks, shown in Tables 5.2, 5.3, 5.4, and 5.5. All of the trumpets have moderate mean scores, and their rankings do not agree with the expected scores from the modeling.

Participant	Trumpet Y ranking	Trumpet S1 ranking	Trumpet S2 ranking	Trumpet B ranking
1	4	3	2	1
2	2	1	4	3
3	1	2	4	3
4	4	3	2	1
5	1	4	3	2
Mean	2.4	2.6	3	2
Standard deviation	1	1.14	1.52	1
Expected from modeling	1	3	2	4

Table 5.2: Results for Task 2 of the perceptual trial. Each instrument is ranked by each player in order from the instrument on which they could diminuendo the least (1) to the instrument on which they could diminuendo the most (4) after a minimum-pressure onset.

Participant	Trumpet Y ranking	Trumpet S1 ranking	Trumpet S2 ranking	Trumpet B ranking
1	2	1	3	4
2	4	2	3	1
3	2	1	3	4
4	2	4	1	3
5	2	1	4	3
Mean	2.4	1.8	2.8	3
Standard deviation	0.89	1.3	1.1	1.22

Table 5.3: Results for Task 3 of the perceptual trial. Each instrument is ranked by each player in order from the instrument on which they needed the least blowing pressure (1) to the instrument on which they needed the most blowing pressure (4) to play at their maximum dynamic.

Note that for Task 3, there is no expected ranking with which to compare the results because the question does not directly correlate to any of the values found through numerical continuation.

Participant	Trumpet Y ranking	Trumpet S1 ranking	Trumpet S2 ranking	Trumpet B ranking
1	1	3	2	4
2	3	4	2	1
3	3	1	1	4
4	3	2	1	4
5	3	2	4	1
Mean	2.6	2.4	2.2	2.8
Standard deviation	0.89	1.14	1.1	1.64
Expected from modeling	1	3	2	4

Table 5.4: Results for Task 4 of the perceptual trial. Each instrument is ranked by each player in order from the instrument whose minimum onset attack was the most quiet (1) to the least quiet (4).

Participant	Trumpet Y ranking	Trumpet S1 ranking	Trumpet S2 ranking	Trumpet B ranking
1	2	4	3	1
2	2	3	1	4
3	3	4	2	1
4	4	1	3	2
5	3	4	2	1
Mean	2.8	3.2	2.2	1.8
Standard deviation	0.84	1.3	0.84	1.3
Expected from modeling	3	1	4	2

Table 5.5: Results for Task 5 of the perceptual trial. Each instrument is ranked by each player in order from the instrument on which the note produced sounded the least loud (1) to the most loud (4) when playing at their maximum blowing pressure.

5.3 Discussion and limitations

There are large limitations inherent to this type of perceptual testing, because players are not able to use a measured or controlled level of blowing pressure, and it is very difficult for them to make accurate judgements about their own dynamic levels and blowing pressure.

In general, players were able to detect qualitative differences between the trumpets, but they did not always identify these differences in the same way. For example, all players

commented that Trumpet B, the only student-model instrument, felt much different to play than the other instruments; however, the players were usually divided about which extreme end of the spectrum to place it on. Aside from Task 2, for which players gave Trumpet B more moderate ratings in general, players almost always ranked Trumpet B as either 1 or 4, but the ranking was not consistent between players for each task. The result of this is that it received the most extreme rankings, but the mean ranking was still moderate for all tasks. This implies that players were aware that Trumpet B was different from the other trumpets, but were not able to discern the way in which it was different.

Players also commented throughout the experiment that the professional model instruments, Trumpets Y, S1, and S2, were very similar to one another. There may have also been some influence of how similar each instrument was to the instrument that each player was used to playing, with a similar effect for how similar the mouthpiece was to their usual mouthpiece. Participants 2 and 3 usually play a Bach Stradivarius model 43 instrument, Participant 5 plays a Bach model 37, the same model as Trumpets S1 and S2 (though Trumpet S2 has been modified), and Participants 1 and 4 play on Yamaha instruments that are not the same model as the one used in this experiment. None of the participants were used to playing a Bach 1.5c mouthpiece, though it is a common mouthpiece model and size. Participant 5, the only player who regularly plays one of the trumpet models used for this experiment, stated that they preferred Trumpet S1 in general and that they also thought it was most similar to the one they were used to playing. Players also tended to make comments referring to trumpets as “the best” or “the worst” for a given task, even though these values were not assigned in the description of the task. This implies that the players’ personal preference was a factor in their rankings, and that their rankings may have been influenced by an instrument’s level of similarity to their own

personal instrument.

Chapter 6

Discussion and Conclusions

In this thesis, four trumpets of varying makes and calibres have been compared using numerical continuation methods. Results were produced similar to those found in Fréour et al. [2020], and a small-scale perceptual trial was conducted to attempt to determine whether the conjectures made based on results from numerical continuation are perceptible to players. It was found that there were significant differences between the numerical continuation results for the trumpets, and that they showed a clear pattern. In general, the results for the three professional model instruments, Trumpets Y, S1, and S2, were much closer to each other than to Trumpet B. The results for these instruments were generally more favourable for players; they had a lower onset pressure and dynamic, a lower hysteresis amplitude, a lower extinction dynamic, and a larger dynamic range, though the maximum volume was comparable for all four trumpets. For the values related to the Hopf bifurcation, the fold, and the amplitude of the hysteresis, Trumpet Y had the most favourable results, followed by Trumpets S2, S1, and B. For the p value at maximum blowing pressure and the dynamic range, the most favourable results were for Trumpet S2,

followed by Trumpets Y, S1, and B, though the results were closer together for these factors. It can be concluded that the student-model Besson trumpet showed much less favourable results than the three professional model trumpets, particularly for factors related to the low range of its dynamics. The three professional model instruments were closer to one another, but in general, Trumpet Y showed more desirable results for the low range of dynamics, and Trumpet S2 was more favourable for the louder dynamics, though Trumpets Y and S2 were very close together for all factors.

The perceptual trial was designed to determine whether players could recognize differences between the instruments that correlated with the results from numerical continuation. It was found that there was not a consensus between the players about their rankings for any of the tasks, and that the rankings did not seem to align with the results from the modeling. The most notable observation from the rankings was that players tended to rank Trumpet B as either a 1 or a 4, the two extreme ends of the scale. This implies that the players were able to perceive the difference between the instruments, but not to consistently determine the direction of the difference. This was confirmed by the players' verbal comments that Trumpet B was much different from the other instruments. Most of the players stated that they disliked Trumpet B, but Player 2 preferred it, implying that the players' preferences for the factors studied may not be universal.

6.1 Limitations and future work

One limitation of the research in this thesis is that only one set of lip parameters was tested for each instrument. It was noted in Chapter 4 that the location of the Hopf bifurcation point for Trumpet B seems unreasonable. Velut et al. [2017] found that the optimal lip

frequency value was highly dependent on the choice of lip quality factor Q_l, and a similar phenomenon was observed when different Q_l values were tested to decide what value to use for this thesis. The Q_l value that was used for this thesis was chosen in order to make sure that the desired resonance was excited for each instrument, but the choice was not refined further. It is possible that the results are highly dependent on the lip parameters chosen, though results from testing with varied lip parameters in [Fréour et al., 2020] suggest that the patterns observed between instruments depend more on the measured impedance than on the lip parameters. Testing with varied lip parameters could help determine how sensitive the results are to changes in the lip parameters. It is also important to note that the LSA approach used in this thesis does not consider the effect of changing other lip parameters. For a more thorough analysis of the lip parameters, multiple parameters could be varied simultaneously in order to determine the optimal combination of parameters. This may allow us to determine whether the unusually high oscillation threshold value for Trumpet B was due to the choice of lip parameters.

We also used a simplified, one-dimension lip model for this thesis, though stroboscopic lip measurements in works such as [Copley and Strong, 1996] have suggested that the lips actually vibrate on two axes. Further research could therefore include analysis using a two-dimensional lip model, such as the one used in [Adachi and Sato, 1996], in order to determine whether using a lip model that allows for motion in more directions changes these results considerably.

The methodology used in this thesis could be used to make objective comparisons between existing trumpet models, for use in the design and marketing of instruments. Further work in this area could also involve investigating the correlation between numerical continuation results and observable differences in the instruments' impedances. Modeled impedances

could also be created and modified, using modeling techniques such as transmission matrix modeling, in order to observe how making small changes to the instruments' geometry affects the results from numerical continuation.

In the perceptual experiment, there was a lack of objectivity even though the players could not tell what instrument they were playing visually or tactilely, since they could often recognize which instrument was which just from playing the exercises. They were also influenced by how similar an instrument was to their own instrument, and were not able to control or assess their playing sufficiently to make objective judgements. The players were also not used to making judgements of this type, and expressed that some factors were difficult to discern, or conflated the qualities they were judging with other factors, such as the level of "resistance" they felt from the instrument. Some players also referred to the instruments as "better" or "worse" than one another for a task, assigning judgements of quality that were not indicated in the directions. Some of these issues could be resolved by having a larger-scale experiment, as some of the biases would likely even out with more participants, but in order to resolve more of the difficulties with perception and control, it may be helpful to combine the perceptual study with another type of measurement apparatus, or to perform a different type of experiment altogether. The same type of trial could be used in conjunction with a decibel meter to determine the loudness of the sounds produced, and a device to measure the mouth pressure as in [Fletcher and Tarnopolsky, 1998]. These results could also be tested by running time-domain simulations with the model to see if the results are as expected, as in [Velut et al., 2017], or by setting up an artificial player system with controllable blowing pressure and lip parameters, and measurable output, as in [Petiot et al., 2003].

Bibliography

Frédéric Ablitzer. Peak-picking identification technique for modal expansion of input impedance of brass instruments. *Acta Acustica*, 5(53), 2021.

Frédéric Ablitzer. Peakpickingtools. `https://github.com/FredericAblitzer/PeakPickingTools`, 2022.

Seiji Adachi and Masa-aki Sato. Time-domain simulation of sound production in the brass instrument. *Journal of the Acoustical Society of America*, 97:3850–3861, 1995.

Seiji Adachi and Masa-aki Sato. Trumpet sound simulation using a two-dimensional lip vibration model. *Journal of the Acoustical Society of America*, 99:1200–1209, 1996.

Murray Campbell and Seona Bromage. Experimental investigation of the open area of the brass player's vibrating lips. In *Proceedings - Forum Acusticum 2005*, pages 729–734, Budapest, 2005.

Murray Campbell, Jöel Gilbert, and Arnold Myers. *The Science of Brass Instruments*. Springer, Switzerland, 2021.

Bruno Cochelin, N. Damil, and M. Potier-Ferry. *Méthode Asymptotique Numérique*. Hermes Sciences, Lavoisier, 2007.

Tom Colinot, Louis Guillot, and Jean Kergomard. Direct and inverse Hopf bifurcation in a neutral delay differential equation model of reed conical instrument. In *Proceedings of the 23rd International Congress on Acoustics*, pages 6446–6451, Aachen, Germany, 2019.

David C. Copley and William J. Strong. A stroboscopic study of lip vibrations in a trombone. *Journal of the Acoustical Society of America*, 99:1219–1226, 1996.

Jean-Pierre Dalmont, Joël Gilbert, Jean Kergomard, and Sébastien Ollivier. An analytical prediction of the oscillation and extinction thresholds of a clarinet. *Journal of the Acoustical Society of America*, 118:3294–3305, 2005.

Riccardo Di Federico and Gianpaolo Borin. Synthesis of the trumpet tone based on physical models. *International Computer Music Association*, 1997.

Eusebius Doedel. Lecture notes on numerical analysis of nonlinear equations. `http://indy.cs.concordia.ca/auto/notes.pdf`, 2010. Online; accessed 16 February, 2023.

Benjamin Elie, François Gautier, and Bertrand David. Macro parameters describing the mechanical behaviour of classical guitars. *Journal of the Acoustical Society of America*, 132:4013–4024, 2012.

Neville H. Fletcher and Alex Tarnopolsky. Blowing pressure, power, and spectrum in trumpet playing. *Journal of the Acoustical Society of America*, 105(2):874–881, 1998.

Vincent Fréour, Louis Guillot, and Hideyuki Masuda. Numerical continuation of a physical model of brass instruments: Application to trumpet comparisons. *Journal of the Acoustical Society of America*, 148:748–758, 2020.

Margaret Hopkins. Ma_thesis_2023. `https://github.com/MargaretHopkins/MA_thesis_2023`, 2023.

Sami Karkar. *Méthodes numériques pour les systèmes dynamiques non linéaires: Application aux instruments de musique auto-oscillants*. PhD thesis, L'Université d'Aix-Marseille, 2012.

Sami Karkar, Bruno Cochelin, Christophe Vergez, Olivier Thomas, and Arnaud Lazarus. User guide manlab 2.0. `http://manlab.lma.cnrs-mrs.fr/sites/manlab.lma.cnrs-mrs.fr/IMG/pdf/userguide-3.pdf`, 2011. Online; accessed 5 May, 2023.

Jean-Christophe Le Roux. *Capteur d'impedance: Manuel d'utilisateur*. Centre de Transfert de Technologie du Mans, 20, rue Thallès de Millet, Technopole Université, 72000 Le Mans, France, version 2.2 edition, 2013.

Stephane Lejeunes. Manlab - an interactive path-following and bifurcation analysis software. `http://manlab.lma.cnrs-mrs.fr/spip/`, 2011. Online; accessed 5 May, 2023.

Harold Lloyd Leno. *Lip vibration characteristics of selected trombone performers*. PhD thesis, University of Arizona, 1971.

Esteban Maestre, Gary P. Scavone, and Julius O. Smith. Joint modeling of impedance and radiation as a recursive parallel filter structure for efficient synthesis of wind instrument sound. In *Proceedings of the 21st International Conference on Digital Audio Effects (DAFx-18)*, pages 157–164, Aveiro, Portugal, 2018.

Hossein Mansour, Vincent Fréour, Charalampos Saitis, and Gary P. Scavone. Post-classification of nominally identical steel-string guitars using bridge admittances. *Acta Acustics united with Acustica*, 101(2):394–407, 2015.

Daniel W. Martin. Lip vibration in a cornet mouthpiece. *Journal of the Acoustical Society of America*, 13(3):305–308, 1942.

Rémi Mattéoli, Joël Gilbert, Christophe Vergez, Jean-Pierre Dalmont, Sylvain Maugeais, Soizic Terrien, and Frédéric Ablitzer. Minimal blowing pressure allowing periodic oscillations in a model of brass instruments. *Acta Acustica*, 5(57), 2021.

Jean-François Petiot, Franck Teissier, Joël Gilbert, and Murray Campbell. Comparative analysis of brass wind instruments with an artificial mouth: First results. *Acta Acustica united with Acustica*, 89:974–979, 2003.

Xavier Rodet and Christophe Vergez. Physical models of trumpet-like instruments, detailed behaviour and model improvements. pages 448–453, 1996.

Richard Roy and Thomas Kailath. Esprit-estimation of signal parameters via rotational invariance techniques. *IEEE Transactions on Acoustics, Speech, and Signal Processing*, 37 (7):984–995, 1989.

Hiroki Sayama. *Introduction to the modeling and analysis of complex systems*. Open SUNY Textbooks, Geneseo, NY, 2015.

Fabrice Silva. *Émergence des auto-oscillations dans un instrument de musique à anche simple*. PhD thesis, Université de Provence Aix-Marseille I, 2009.

Lionel Velut. *Contrôle par le musicien des régimes d'oscillation des instruments de la famille des cuivres*. PhD thesis, Aix-Marseille Université, 2016.

Lionel Velut, Christophe Vergez, Jöel Gilbert, and Mithra Djahanbani. How well can linear stability analysis predict the behaviour of an outward-striking brass instrument model? *Acta Acustica united with Acustica*, 103:132–148, 2017.

Hermann von Helmholtz. *On the Sensations of Tone as a Physiological Basis for the Theory of Music*. Dover Publications, Inc., New York, 1954. Translated by Alexander J. Ellis from the 4th German Edition of 1877.

Joe Wolfe. Open vs. closed pipes (flutes vs. clarinets). `https://www.phys.unsw.edu.au/jw/flutes.v.clarinets.html`. Online; Accessed 26 May, 2023.

Jim Woodhouse. On the playability of violins. Part II: Minimum bow force and transients. *Acta Acustica united with Acustica*, 78(3):137–153, 1993.

Shigeru Yoshikawa. On the modeling of self-oscillation in brass instruments. *Journal of the Acoustical Society of America*, 84:449–451, 1988.

Shigeru Yoshikawa. Acoustical behaviour of brass player's lips. *Journal of the Acoustical Society of America*, 97:1929–1939, 1995.

Shigeru Yoshikawa and George R. Plitnik. A preliminary investigation of brass player's lip behavior. *Journal of the Acoustical Society of Japan*, 14:449–451, 1993.

Appendix A

Plots of modal impedance fits

The impedance curves generated using the fitted modal parameters are plotted along with the measured impedances for all four trumpets in Figures A.1, A.2, A.3, and A.4. The residuals for each fit are plotted below in black. In each plot, the modal fit closely follows the measured impedance, though some peaks are slightly higher or lower, and the fitted curve stops being close to the measured one close to the peak between 800 and 1000 Hz because only the first seven peaks in the data were fitted. This region of the data encompasses the majority of the range played on the trumpet, and is sufficient for studying the trumpet's fourth resonance, between 400 and 500 Hz. The first impedance peak around 150 Hz, which is for the pedal tone of the instrument, is outside of the relevant range for this research and is not included in the measured data.

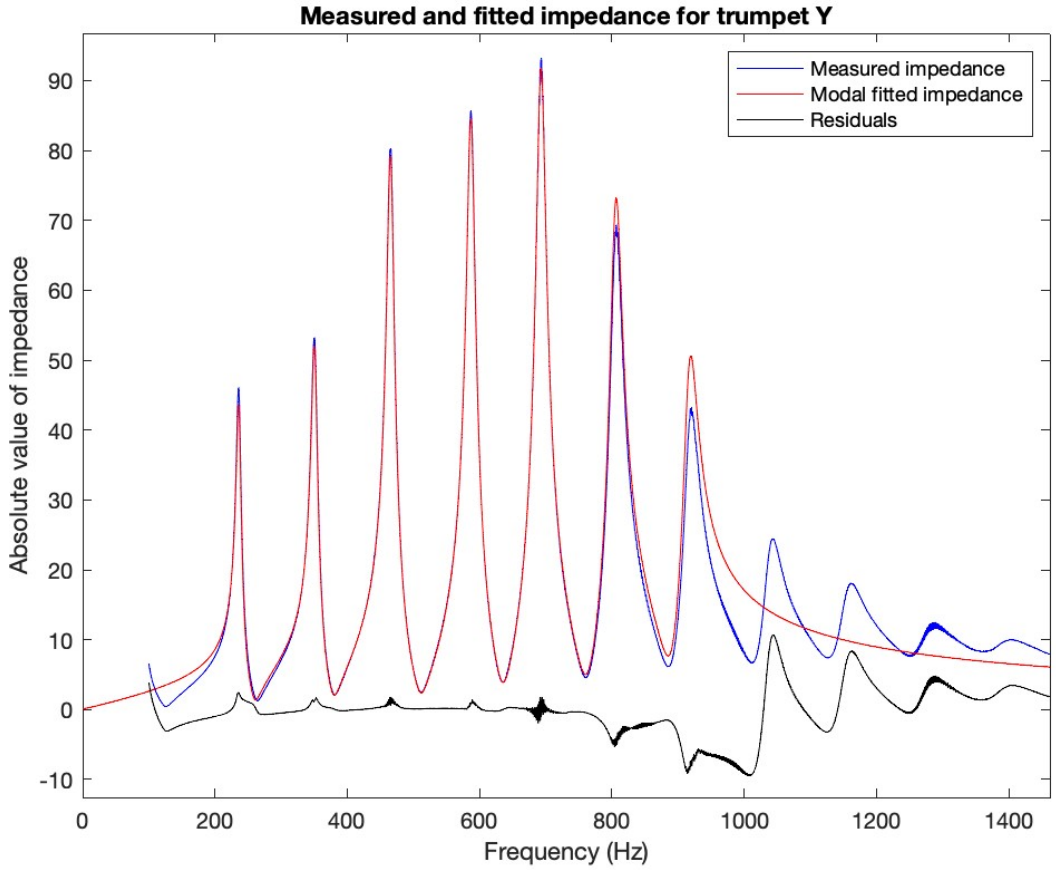

Figure A.1: Impedance plot for Trumpet Y, including the measured impedance in blue, the fitted impedance in red, and the residuals in black.

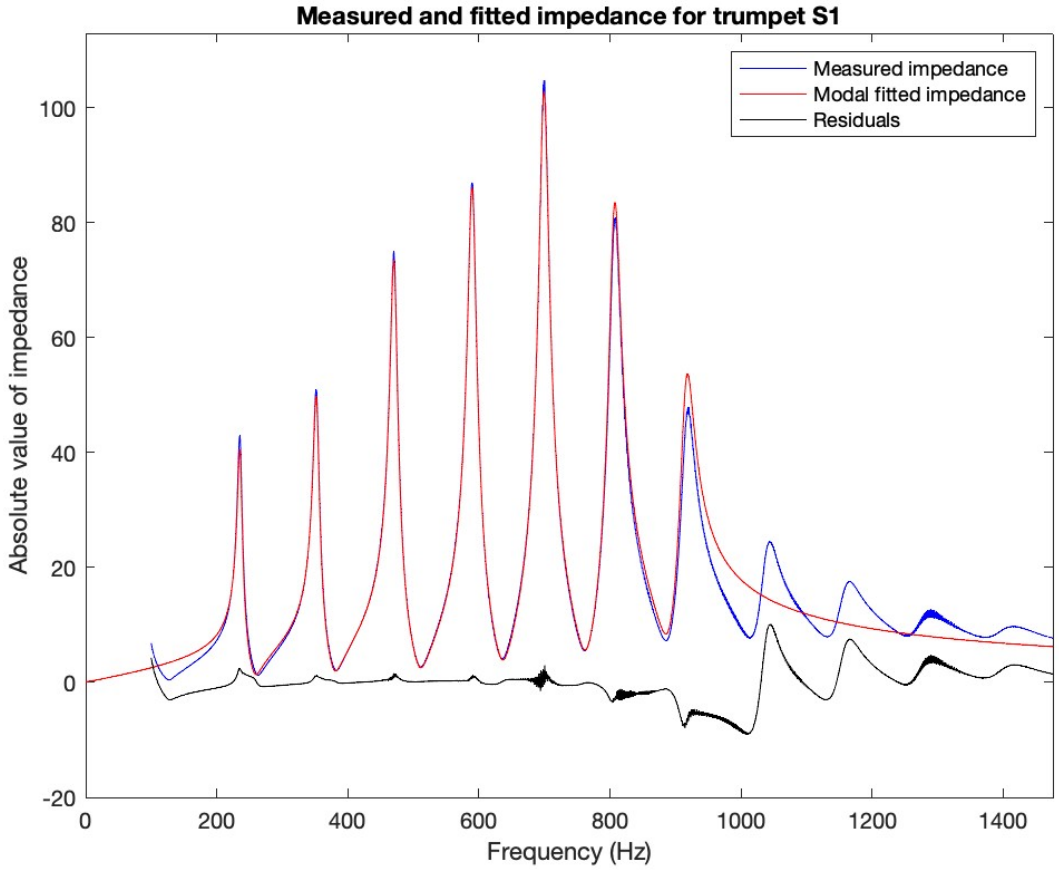

Figure A.2: Impedance plot for Trumpet S1, including the measured impedance in blue, the fitted impedance in red, and the residuals in black.

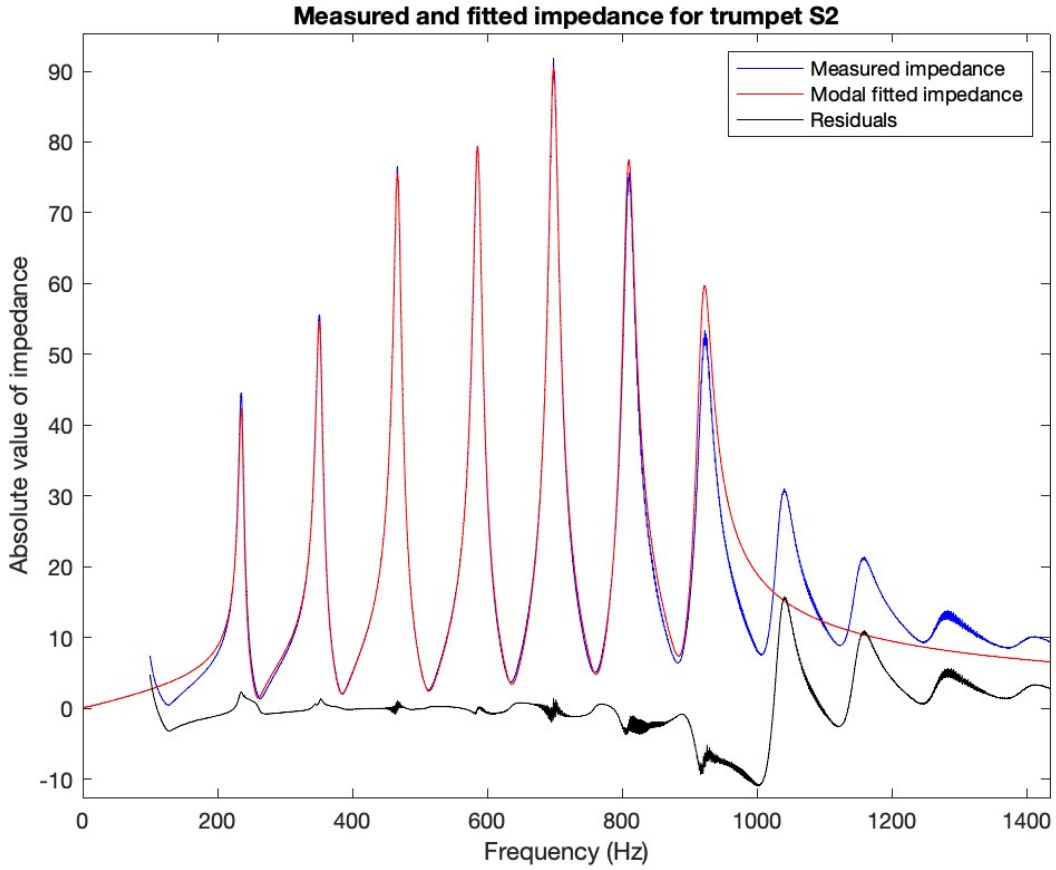

Figure A.3: Impedance plot for Trumpet S2, including the measured impedance in blue, the fitted impedance in red, and the residuals in black.

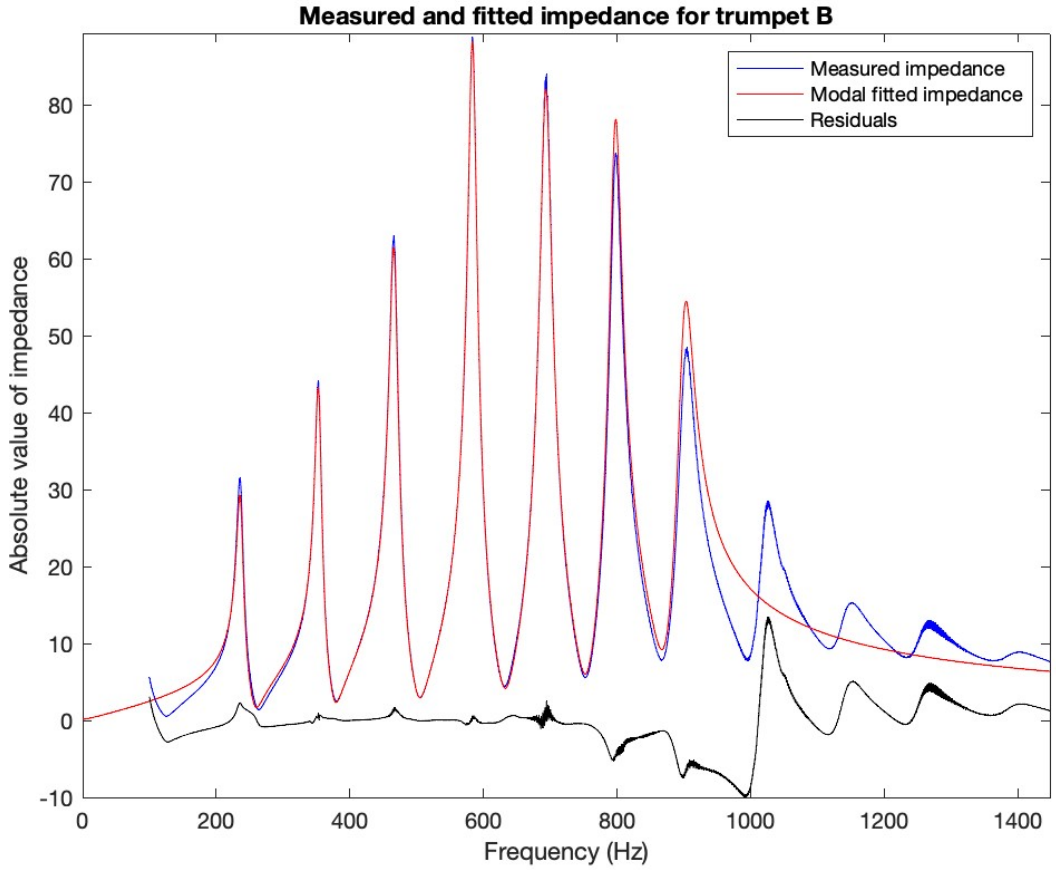

Figure A.4: Impedance plot for Trumpet B, including the measured impedance in blue, the fitted impedance in red, and the residuals in black.